Particle Physics at CERN

Annual Report 2007

(SNF grants 200020-115960 and 206620-115962)

E. Alagöz, Y. Allkofer, C. Amsler, A. Benelli, V. Boccone, H. Cabrera, V. Chiochia, S. Horikawa, Hp. Meyer, C. Regenfus, P. Robmann, J. Rochet, T. Rommerskirchen, A. Schmidt, T. Speer, S. Steiner, M. Thomann, D. Tsirigkas, and L. Wilke.

Secretariat: P. Perréard

April 29, 2008

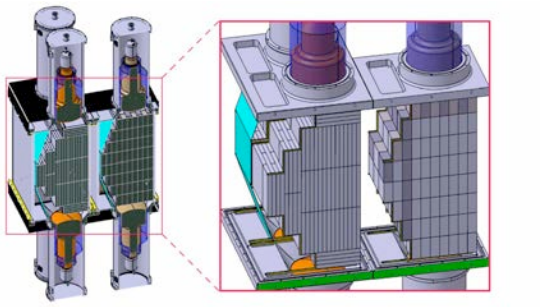

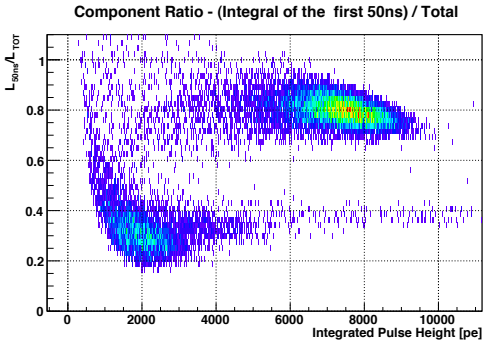

Physik-Institut der Universität Zürich
Winterthurerstrasse 190, CH-8057 Zürich, Switzerland

Contents

1 Search for $K\pi$-atoms **3**

2 Search for dark matter with liquid argon **7**

3 Particle physics with CMS **11**

4 Publications **16**

This report covers the activities of the Zurich group at CERN on the CMS, the DIRAC and the ArDM experiments between 1 April 2007 and 31 March 2008. It does not include the activity of C. Amsler contributing to the "Review of Particle Physics" (Particle Data Group). Further details on the group activities and publication reprints can be obtained from our home page, see http://www.cern.ch/unizh/.

1 Search for $K\pi$-atoms

Y. Allkofer, C. Amsler, A. Benelli[1], S. Horikawa, C. Regenfus, and J. Rochet

In collaboration with:
Basel, Bern, Bucharest, CERN, Dubna, Frascati, KEK, Kyoto, Messina, Moscow, Prague, Protvino, Santiago and Tokyo.

(DIRAC-II Collaboration)

The $K\pi$-scattering length is of interest to test chiral perturbation predictions involving the s-quark. The low energy $K\pi$-phase shifts (S-wave isospin 1/2 and 3/2 phases) are poorly known below 1 GeV/c and hence their extrapolations to zero energy are very uncertain. We are therefore searching for the electromagnetically bound $K^+\pi^-$ (and $K^-\pi^+$) system to measure its mean life τ which is related to the S-wave $K\pi$-scattering length. We intend to measure τ (predicted to be about 3.7 fs) with a precision of 10%.

Details on the DIRAC apparatus can be found in ref. [1]. We have developed and built the aerogel Čerenkov counters and the heavy gas system required to identify kaons from the dissociation of $K\pi$-atoms, and are responsible for the analysis of the corresponding data. More on these detectors can be found in previous annual reports and in a recent publication [2].

The aerogel detector is located in the left (positive charge) arm of the DIRAC spectrometer and consists of three independent modules. Two of them have aerogel with the refractive index $n = 1.015$ (24ℓ) for kaon-proton separation between 4 and 5.5 GeV/c , and the third one (13ℓ) has the lower index $n = 1.008$ for 5.5 to 8 GeV/c kaons. The loss due to light absorption is compensated by using a wavelength shifter and also by increasing the radiator thickness at the center of the detector (pyramid geometry). A cosmic ray test showed that, thanks to the pyramid design, the light yield did not depend significantly on the impact position. For the 1.015 detector we obtained about 6.4 photoelectrons for cosmic muons, implying ~ 5 photoelectrons for 4 GeV/c kaons. The performance of the 1.008 counter could not be tested with cosmic rays.

Figure 1.1: *Photographs of the three aerogel modules (black) in the experimental area. The scintillation hodoscopes and the N_2-Čerenkov counter (blue) are also visible.*

[1] Visitor from the University of Basel

Figure 1.1 shows the aerogel counters installed in the DIRAC experiment in the West hall at CERN. The operation of the DIRAC-II experiment, originally planned for summer 2006, was postponed by one year due to repeated failures of a switching magnet in the CERN primary proton beam line. The defective magnet was successfully replaced by CERN in spring 2007 and DIRAC-II could finally be commissioned in June 2007. The aerogel counters worked in the beam according to expectations, although we had first to strengthen the magnetic shielding of the (vertical) photomultipliers with additional μ-metal to protect them from the fringe field of the DIRAC dipole magnet, which is also vertical.

The trigger rejects electrons with the N_2-Čerenkov detector in anticoincidence and selects symmetric tracks in the two spectrometer arms. Mainly pions and protons are present, as well as a few kaons. The pions are shown by the green ellipse and protons by the red ellipse in fig. 1.2 (left). The horizontal accumulation of events at low amplitudes (blue ellipse) is due to the ADC pedestals for triggers with protons below Čerenkov threshold, including electronic noise. Kaons are not visible at this point due to their low intensity.

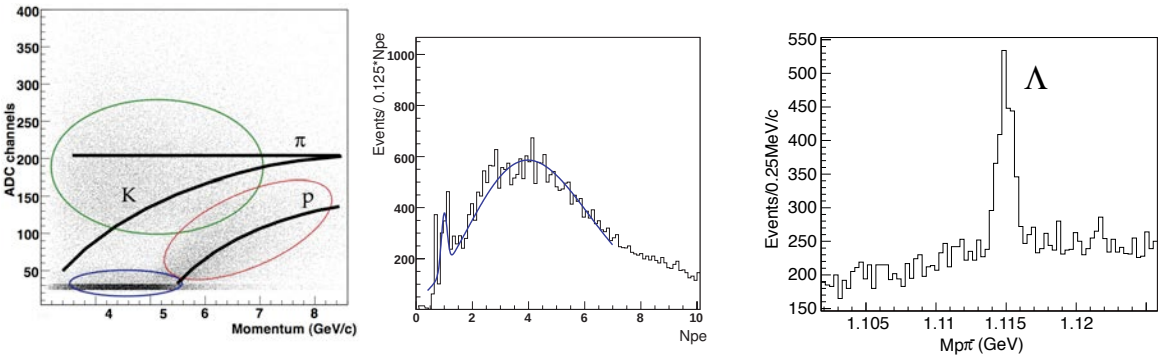

Figure 1.2: *Left: signal amplitude (in ADC counts) as a function of momentum for one of the $n = 1.015$ aerogel modules. The curves show the expected light yields as a function of momentum. The ellipses show the pions (green), the protons (red) and the electronics noise (blue). Middle: distribution of the light output (in photoelectrons, N_{pe}) for positive kaons traversing the heavy aerogel counter (see text). The curve is a fit. Right: Λ-signal in the $\pi^- p$-invariant mass distribution.*

Data were also taken with inverted polarities to study the proton contamination, i.e. by triggering on negative tracks in the aerogel arm, in which case the contribution from antiprotons is negligible. The normalized ADC spectra were then subtracted, leaving essentially protons in the positive charge spectrum which was then subtracted from the distribution shown in fig. 1.2 (left), leading to a pure K^+-spectrum. Figure 1.2 (middle) shows the distribution of the light amplitude which agrees with cosmic ray measurements. The peak at low amplitudes is due to the one-photon contribution. Cutting at one photoelectron one obtains a proton rejection efficiency of about 93.2%, while the kaon detection efficiency is 94.2%. The proton contribution can also be studied with $\Lambda \to \pi^- p$ decays (see fig. 1.2, right).

We have also built the C_4F_{10} heavy gas system for the Čerenkov counters in both arms to veto pions. The counters were delivered by our collaborators from Dubna. The system has been running since June 2007 without interruption. However, the rate of C_4F_{10} loss was found to be larger than initially estimated and be modified. The design of the improved scheme has been done (fig. 1.3) and

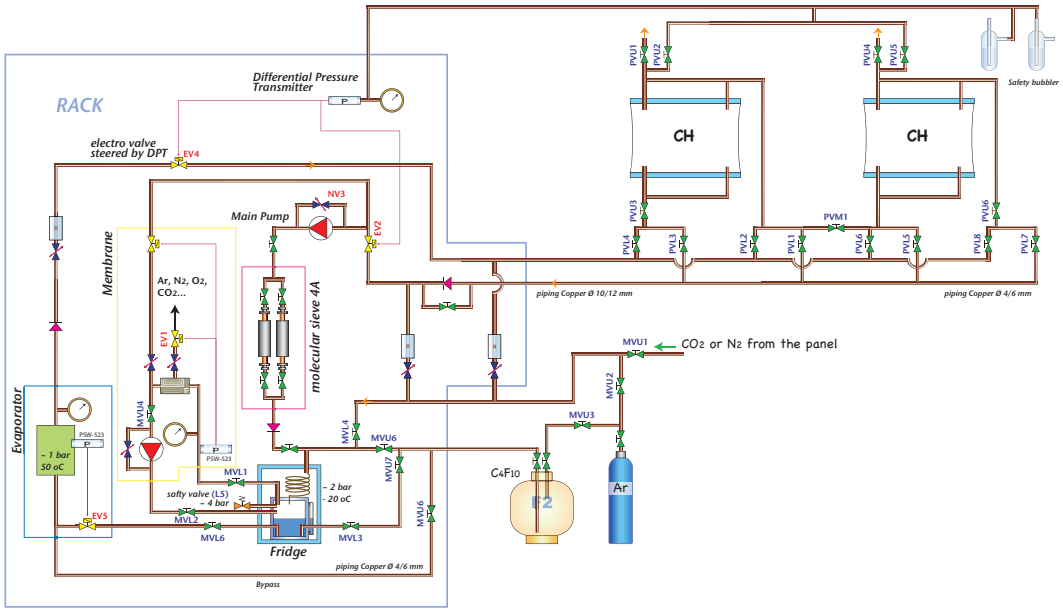

Figure 1.3: *Diagram of the radiator-gas recirculation system built by our group (improved in robustness for the DIRAC-II 2008 runs).*

the construction will be completed for the 2008 runs.

Figure 1.4 (left) shows an amplitude spectrum for electrons from the C_4F_{10}-detector, obtained by triggering on the N_2-Čerenkov counter. Dividing the mean amplitude by that of the single-photoelectron peak, we obtain the mean number of photoelectrons $N_{\rm pe} = 28.0 \pm 0.2$. Figure 1.4 (right) shows the signal amplitude for pions as a function of momentum. The curve is a fit in which the refractive index of the radiator and the number of photoelectrons were set as free parameters, assuming a velocity $\beta = 1$. The fit leads to a refractive index $n = 1.00137$ which corresponds to a wavelength of 300 nm for Čerenkov photons and is consistent with the Čerenkov spectrum convoluted with the spectral response of the UV-glass photomultiplier. The pion detection efficiency is found to be larger than 99.5% at 4 GeV/c.

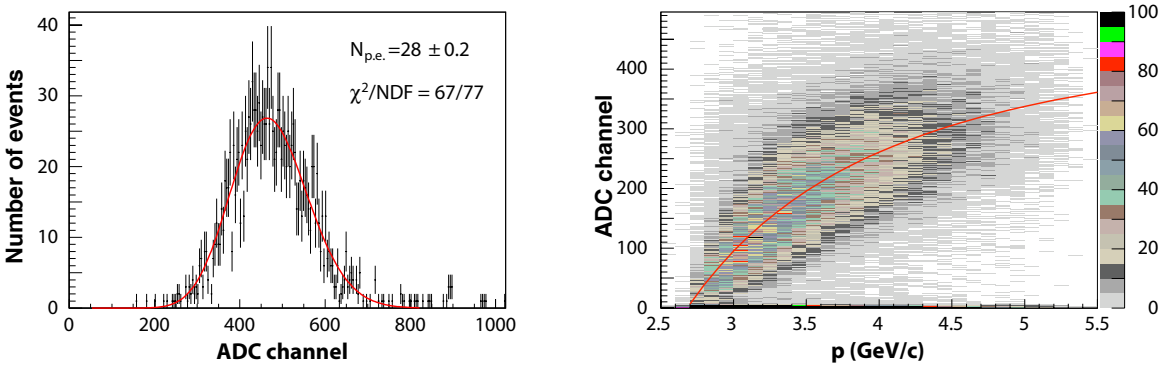

Figure 1.4: *Left: amplitude spectrum of electrons in the heavy gas counter. Right: pulse height distribution for pions as a function of momentum.*

The yield of $K\pi$- atoms is expected to be about 25 $\times$ lower than for $\pi^+\pi^-$-atoms [3]. Assuming equal acceptances and the increase in beam flux between the former DIRAC I experiment (which studied $\pi^+\pi^-$-atoms) and DIRAC II by a factor of two, this should lead to about 1'400 reconstructed $K^+\pi^-$- (and $K^-\pi^+$-) atoms in the 2007 sample. DIRAC II will take data at least until the end of 2009.

References

[1] B. Adeva *et al.*, Nucl. Instr. and Meth. in Phys. Research **A 515** (2003) 467
[2] Y. Allkofer *et al.*, Nucl. Instr. Meth. in Phys. Research **A 582** (2007) 497
[3] B. Adeva *et al.* (DIRAC Collaboration), Phys. Lett. **B 619** (2005) 50

2 Search for dark matter with liquid argon

C. Amsler, V. Boccone, H. Cabrera[2], S. Horikawa, C. Regenfus, J. Rochet and M. Thomann[3]

In collaboration with:
CIEMAT, ETHZ, Soltan Institute (Warsaw), Universities of Granada and Sheffield

(ArDM Collaboration)

We are building a one ton liquid argon time projection chamber to detect recoil nuclei from the scattering of Weak Interacting Massive Particles. WIMPs (in particular the lightest supersymmetric particle, the neutralino), are among the favorite candidates for the missing non-baryonic matter in the universe. Details on the experiment can be found in our previous annual reports.

In 2007 the Zurich group concluded its laboratory development program for the light readout system and the ArDM collaboration started to assemble the full-scale one ton apparatus. A sketch of the detector is shown in fig. 2.5 (left). The working principle is as follows: in liquid argon a WIMP collision leading to 30 keV nuclear recoils produces about 400 VUV (128 nm) photons, together with a few free electrons. The latter are drifted in a strong vertical electric field and are detected in the gas phase by a large electron multiplier above the surface of the liquid, while the VUV scintillation light is shifted into blue light by a wavelength shifter (WLS) and detected by cryogenic photomultipliers at the bottom of the vessel.

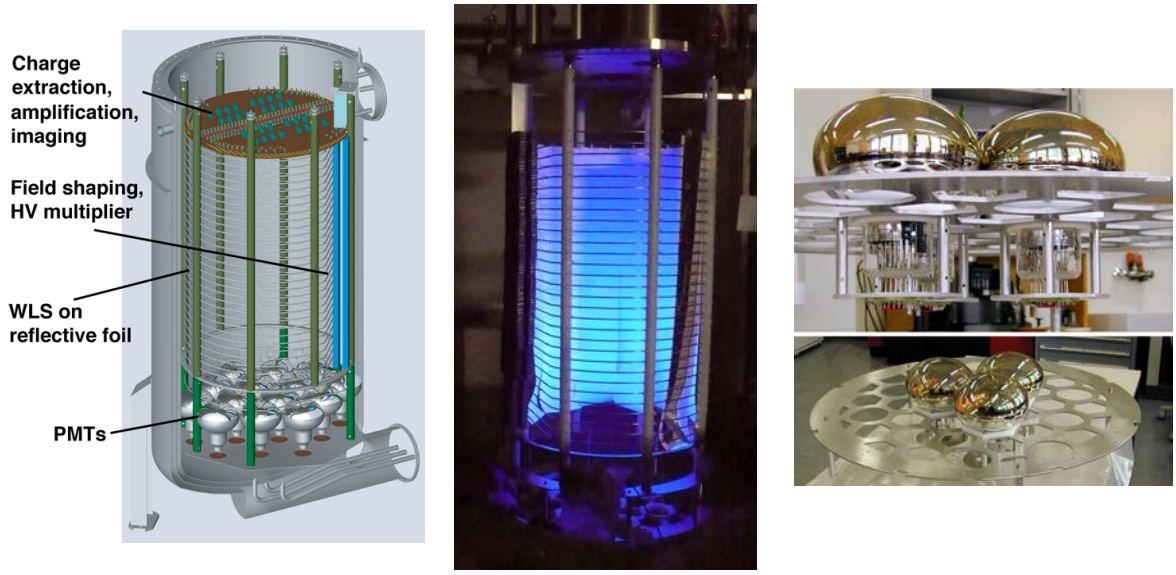

Figure 2.5: *Left: sketch of the ArDM detector. Middle: HV divider, WLS foils and photomultipliers (PMT) under UV illumination. Right: PMT support structure built by our group with three of the fourteen 8" (Hamamatsu R5912-MOD) PMTs.*

From extensive tests performed by our group we concluded that the highest light collection efficiency would be achieved with WLSs made of a 254 μ thick Teflon fabric (Tetratex) coated with

[2]Master student
[3]Bachelor student

$\approx$1 mg/cm^2 tetraphenyl butadiene (TPB) [1] (see below). We constructed a large evaporation chamber capable of coating a 1.4 m long and 0.3 m wide sheet of Tetratex. Twelve sheets were coated to cover the cylindrical side walls inside the electric field shapers (fig. 2.5, middle). The light detection system consists of fourteen 8" hemispherical PMTs in a staggered arrangement at the bottom of the vessel (fig. 2.5, right). We have investigated PMTs for their functionality and quantum efficiency at low temperature. The best result was obtained with Hamamatsu PMTs (R5912-MOD) manufactured with Pt-underlay. A light but sufficiently strong mechanical support was constructed to withstand the buoyant force ($\approx$ 1kN) acting on the PMTs in liquid argon. Eight PMTs were installed for readout tests. The PMT glass was coated with a thin wavelength shifting layer of a transparent TPB-paraloid compound to increase the VUV light yield. Vacuum feedthroughs, cables for the high voltage and signal lines were installed, as well as parts of the data acquisition system.

The ratio of primary scintillation light to ionization charge collected after a given drifttime in an external electric field is different for nuclear recoils and minimum ionizing particles, being very high for the former, due to quenching. This provides the main discrimination between WIMPs and background. In liquid, on the other hand, the VUV photons are produced by ionization from the spin singlet and triplet states of the excited dimer A_2^* which have different lifetimes (τ = 7 ns, resp. 1.6 μs in liquid). These states are populated differently according to the excitation process: for heavy ionization (such as nuclear recoils) the singlet dominates, while for minimum ionizing particles (such as electrons) the triplet dominates. Hence the discrimination of decay time allows a further separation between WIMP induced recoils and background from γ or electrons.

A considerable effort was devoted in 2007 to measure the mean decay lives of the fast (12 ns) and slow (3.2 μs) components of argon luminescence in argon gas at NTP (which are different from liquid) and to determine the population ratio between the slow and fast components. We used a ^{210}Pb-source emitting 5.3 MeV α-particles and 1.2 MeV electrons. This work initiated in ref. [2] is the subject of a recent publication [3]. Figure 2.6 (left) shows for instance that the mean life of the slow component strongly depends on argon purity.

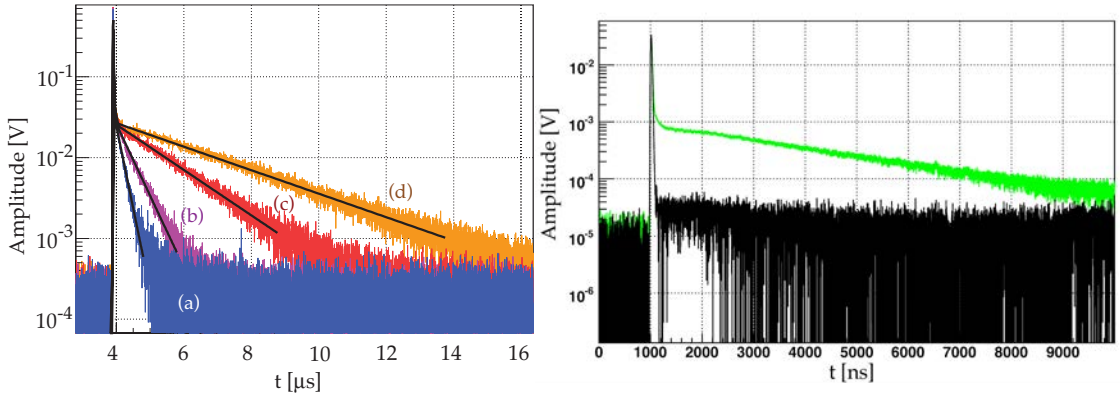

Figure 2.6: *Left: time distribution from an α-source in gaseous argon as a function of contaminating residual air pressure for 10^{-2} (a), 10^{-3} (b), 2.3×10^{-4} (c) and 10^{-5} mbar (d) (from [3]). Right: time distribution without (green) and with (black) absorbing quartz plate.*

We have also determined that the fast decaying component in gaseous argon at NTP stems from UV-light from the so-called [4] third continuum above 160 nm, while the slow component is due to

128 nm photons from the second continuum. This appears to be in contrast to liquid in which both components are due to 128 nm VUV-photons. The measurement was performed by inserting a thin quartz plate in front of the PMT photocathode to absorb radiation below 200 nm. Figure 2.6 (right) shows that the fast component is not affected, while the slow component is absorbed [3].

Similar measurements were made in liquid argon [5]. In liquid we noticed that the light yield was slowly decreasing with time after liquefaction. However, the decay time of the second component (τ = 1.6 μs) was not affected. The origin of this effect is not understood yet, but could be interpreted either as due to the slow cooling of the dynodes (poor heat conductance of the PMT leads) or due to impurities which are absorbing the UV-light.

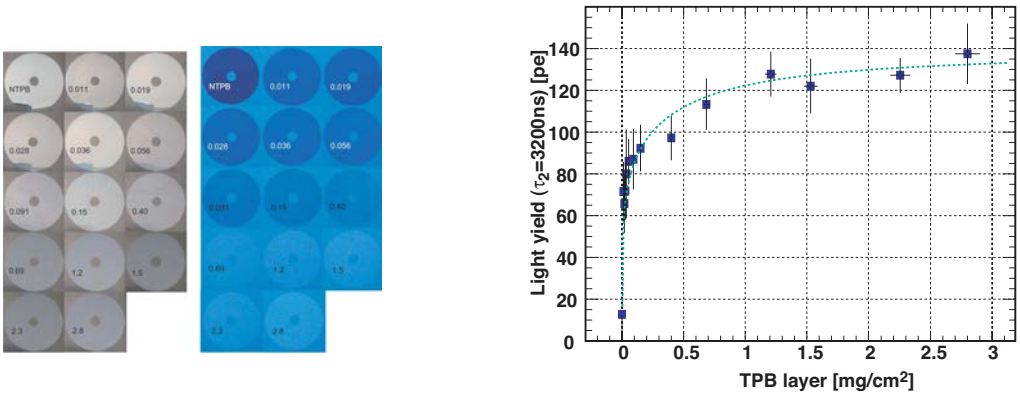

Figure 2.7: *Left: disks of ESR-foils covered with TPB under ambient and UV light. Right: number of photoelectrons (pe) as a function of WLS thickness.*

We also measured the light yield dependence on the WLS thickness of evaporated specular reflectors foils. The measurements were made with a small cell containing gaseous argon at atmospheric pressure. Two materials were selected, Tetratex and ESR-foils from 3M, and the optimum thickness of the TPB layer on the reflector was determined experimentally [1]. The best conversion efficiency, uniformity and reproducibility were achieved by evaporating TPB on the reflector. Several disks of ESR foils (diameter 70 mm) were covered with TPB layers of different thicknesses. The TPB thickness was determined by weighing the disks before and after evaporation. The increase in brightness with TPB thickness is apparent under UV illumination (300 nm) (fig. 2.7, left). The response to 128 nm light was determined using scintillation light from gaseous argon and an α-source. The light yield of the slow component (3.2 μs in gas) is shown in fig. 2.7 (right) as a function of thickness. The data are consistent with a saturation of VUV conversion efficiency above 1 mg $\cdot$ cm^{-2}. Tetratex coated with 1 mg $\cdot$ cm^{-2} TPB was finally chosen for the one ton detector.

As mentioned above, impurities in argon strongly reduce the lifetime of the slow scintillation component. We have therefore built a liquid-argon purity monitor based on the measurement of the lifetime of the triplet excimer state. A small liquid argon cell containing a ^{210}Pb-source emitting both α and β is viewed by a photomultiplier with MgF_2 window and CsTe photocathode which is sensitive to 128 μm VUV-photons (quantum efficiency $\sim$ 20%). Figure 2.8 (left) shows the correlation between the fraction R of the fast ($<$ 50 ns) scintillation component and the total pulse height. The α-signal is clearly separated from the β-signal and noise. The decay time distribution is shown in fig. 2.8 (right) for α-particles. A simple exponential fit leads to a mean life of $\sim$ 470 ns for the slow component

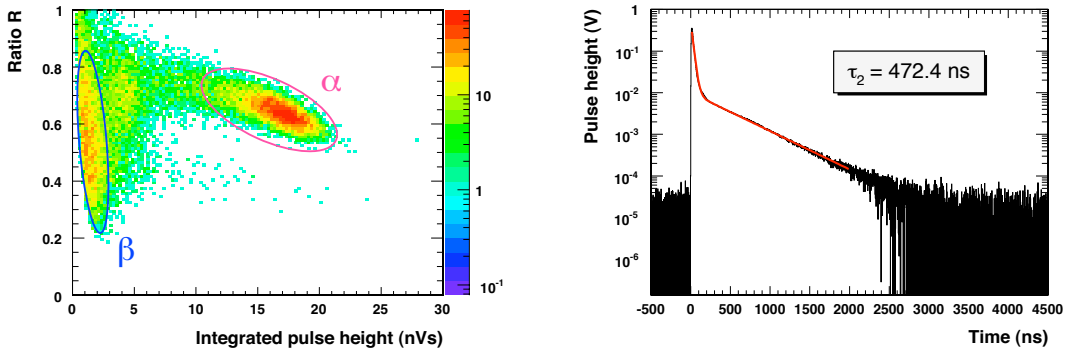

Figure 2.8: *Left: ratio of the fast (<50 ns) signal to the total signal in liquid argon vs. total signal in the purity monitor. Right: decay time distribution for α-particles.*

(while 1.6 μs is expected) and hence indicates a sizeable impurity contamination in the liquid.

The ArDM detector is being assembled at CERN for preliminary readout measurements. We envisage to first install the detector in one of the former LEP pits (OPAL area) for background studies, before moving to a deep underground site.

References

[1] H. Cabrera, Master Thesis, Universität Zürich (2007)
[2] A. Büchler, Bachelor Thesis, Universität Zürich (2006)
[3] C. Amsler *et al.*, Journal of Instrumentation **3** (2008) P02001
[4] W. Krötz *et al.*, Phys. Rev. **A 43** (1991) 6089
[5] M. Thomann, Bachelor Thesis, Universität Zürich (2008)

3 Particle physics with CMS

E. Alagöz, C. Amsler, V. Chiochia, Hp. Meyer, C. Regenfus, P. Robmann, J. Rochet,
T. Rommerskirchen, A. Schmidt[4], T. Speer[5], S. Steiner, D. Tsirigkas, and L. Wilke

In collaboration with:
ETH - Zürich, Paul Scherrer Institut (PSI) and the CMS Collaboration

We have been involved in the design, construction and test of the CMS barrel pixel detector since many years. In particular, we have conducted various performance tests on beams at CERN [1]. The position resolution, the Lorentz angle and the detection efficiency were determined on highly irradiated pixel prototypes. We also deliver the offline software for reconstructing and simulating hits and tracks in the CMS pixel (and strip) detectors, and contribute to the data quality monitoring and alignment codes. The group is furthermore active in the development of algorithms required to efficiently tag B-hadrons, using the pixel vertex detector. The year 2007 and early 2008 were dedicated to the completion of the pixel hardware and to the preparation of the software for data taking and data analysis.

The pixel detector is currently being completed in our institute and at PSI. The institute's workshop manufactured the two detector support structure half-shells for the pixel detector. Figure 3.9 (left) shows the third layer of the final support structure with the mounted pixel detector modules. The production of the final supply tube half-shells is also completed. The electrical power and control lines, the optical signal lines and the cooling fluid are transferred across the supply tubes to the pixel detector. Figure 3.9 (right) shows a supply tube half-shell. The structure consists of thin stainless steel tubes and inner and outer aluminium flanges. The tubes supply the detector with the cooling fluid. The gaps are filled with foam. The power and slow control leads are embedded in the supply tube body. Our electronics workshop manufactured all parts and the detector front end control system. The system consists of four communication and control unit boards, each controling a quarter of the detector with eight barrel readout sectors.

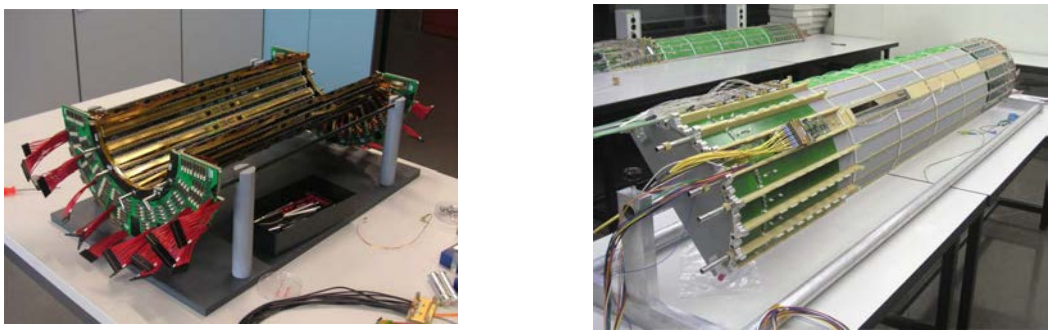

Figure 3.9: *Left: support structure of the third (outer) layer with pixel detector modules. Right: supply tube half-shell during the installation of the electronics boards, the optohybrids and optical fibres. A fully equipped half-shell can be seen in the back.*

A final pixel sensor test had been performed at CERN in autumn 2006. We used a beam telescope with four pixel sensors, two in front and two behind the pixel sensors under test. The 52 $\times$ 80 pixel

[4]Since 1 September 2007
[5]Until 31 August 2007, now at Brown University

device had the final CMS dimensions $150 \times 100\ \mu\mathrm{m}^2$ with a thickness of 285 μm. They were bump-bonded to final CMS pixel readout chips. A PIN diode ($3 \times 6\ \mathrm{mm}^2$) was used as a trigger. Irradiated sensors were kept at $-10^{\circ}\mathrm{C}$ in a cooling box with two Peltier elements. The experimental setup was placed in a Helmholtz superconductor magnet, providing a transverse field of 3T, and was exposed to a 150 GeV π^- beam. Data were taken with and without magnetic field for several bias voltages. The purpose of the test was to compare real data with the predictions obtained from our previous runs which used pixels of different dimensions and a magnetic field parallel to the incident pions [2].

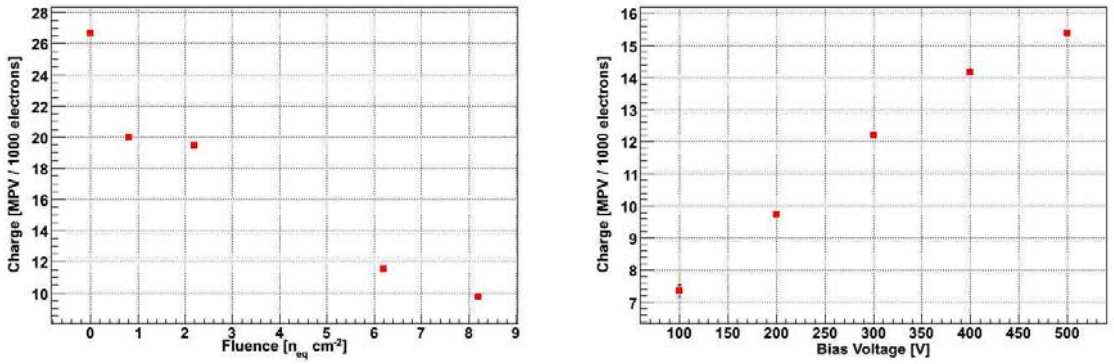

Figure 3.10: *Left: charge collection efficiency for unirradiated and irradiated pixel sensors at 200 V, as a function of fluence. Right: charge collection efficiency for heavily irradiated pixel sensors ($8 \times 10^{14}\mathrm{n_{eq}cm^{-2}}$) as a function of bias voltage.*

The analysis of these data was performed in 2007, involving in particular a careful alignment procedure of the detectors to obtain the best possible resolution in the measurement of the directions of the incident pions. The charge collection in the test module is shown in fig. 3.10 (left) for several irradiatied and unirradiated samples at 200 V bias. One observes a decrease of the collected charge for higher irradiation fluences. The collected charge is reduced to 46 $\%$ for fluences of $6.2 \times 10^{14}\mathrm{n_{eq}cm^{-2}}$ which will be absorbed by the CMS pixel sensors after two years of run at full LHC luminosity. The collected charge is reduced by defects due to radiation damage, which work as charge trapping centers. The charge loss is larger in the magnetic field since the drift length of the electrons increases due to Lorentz deflection. Increasing the bias voltage can recover some of the lost charge (fig. 3.10, right), however at the expense of a reduced drift path, and hence reduced charge sharing, which in turn decreases the accuracy of the position resolution.

Several new features have been implemented in the pixel software, such as a precise description of the material thickness, especially in the complicated regions of the pixel endcaps. Online pixel calibration runs will provide in real time gain response functions for each channel. The size of the calibration tables was reduced substantially to comply with the memory requirements of the CMS reconstruction programs. Detailed simulations have shown that such reductions will have negligible effects on position resolution and b-tagging efficiency.

The alignment of the tracking detectors is a major challenge in the early phase of the experiment. Tracker misalignment (e.g. due to imprecise mounting of sensors or moving structures due to thermal and magnetic field effects) will impair the hit, track and vertex reconstructions, and will decrease the b-tagging efficiency. We have developed a simple algorithm relying on the presence of a secondary vertex and taking the separation between primary and secondary vertex as discriminator. This algo-

rithm does not require a dedicated calibration, is simple and robust enough to be used in the early stage of the experiment. However, the secondary vertex finding efficiency is only 55%. The detector alignment procedure will quickly improve as soon as data from resonances such as J/ψ and gauge bosons become available.

We made important contributions to track reconstruction and b-flavour tagging in fast simulation and are responsible for the interface and maintenance of the b-tagging algorithms in a fast simulation software. Figure 3.11 demonstrates the impressive agreement in terms of b-tagging efficiency and charm mistagging rate, comparing fast and full detector simulations.

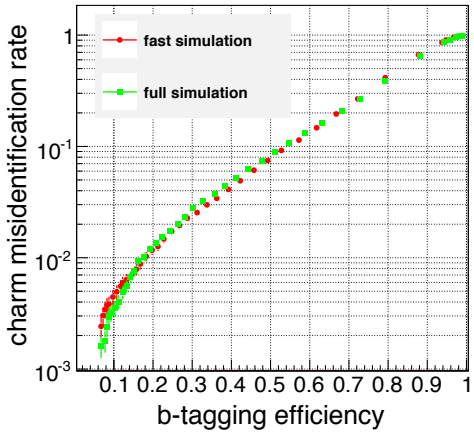

Figure 3.11: *Charm mistagging rate vs. b-tagging efficiency in fast and full detector simulations.*

In the pixel sensors the electrons produced by ionizing particles experience a Lorentz force and drift perpendicular to the 4T magnetic field and the bias electric field. This leads to a shift in the measured coordinates which can be up to 120 μm. This shift has been measured for unirradiated sensors. However, during LHC operation the bias voltage will be increased to compensate for radiation damage (see fig. 3.10) and hence the Lorentz deflection angle will decrease. Furthermore, each detector module will have a different evolution due to non uniform irradiation. Therefore the Lorentz drift needs to be monitored directly from data. Figure 3.12 (left) shows a simulation of the coordinate shift d as a function of depth z in the pixel sensor at which the charge was produced. The average shift can be determined for a given depth with a large number of well-measured tracks (fig. 3.12, right). The slope is the tangent of the Lorentz angle. Such a measurement is done independently for the eight module rings in the three detector layers. Studies for different input values of the Lorentz angle in the detector simulation were performed, as well as studies on the influence of misalignment.

During the first two years of LHC operation we will concentrate on b-physics issues which can be performed at low luminosity. In particular, we will study the decay $B_s^0 \to (J/\psi)\phi \to \mu^+\mu^- K^+ K^-$ and measure the lifetimes of the CP-eigenstates B_s^H and B_s^L. This channel has been chosen as a benchmark channel by the CMS collaboration [3]. A dedicated trigger for B-mesons decaying into two muons via a J/ψ intermediate states was developed, based on the long time of flight of the B-mesons. The secondary vertex of the two muons is reconstructed applying quality cuts on the decay length significance, and on the invariant mass of the two muons. We developed an analysis strategy for the first 100 pb^{-1} expected at the LHC in 2009. The first step is to measure the detector performance using the well known channel $B_d \to J/\psi K^* \to \mu^+\mu^- K^+\pi-$. This channel has very

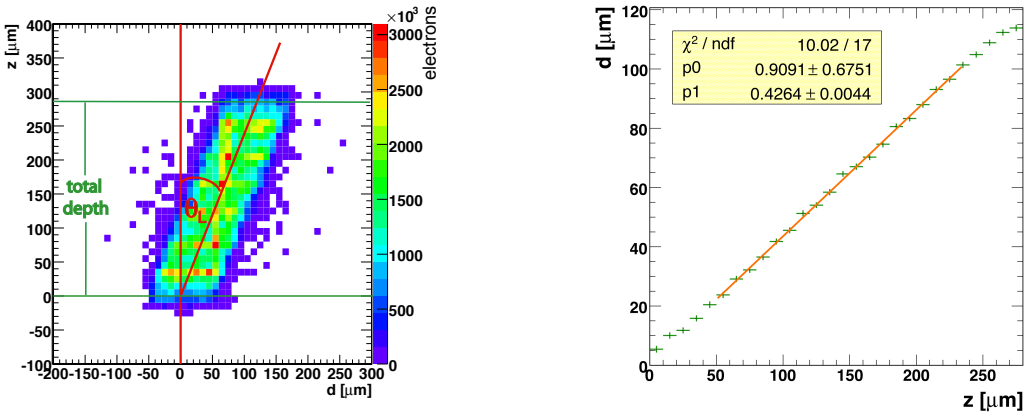

Figure 3.12: *Left: depth z at which the drift electrons were produced vs. readout coordinate d (simulation for muon tracks crossing the pixel detector at a pseudorapidity $\eta = 2$). Right: average drift of electrons d as a function of the production depth z in the silicon sensor bulk. The solid line shows the fit.*

similar properties as the B_s-channel and all parameters have been measured to high precision by BaBar and Belle.

We are also preparing a search for supersymmetry which might be observed early at the LHC. A prominent signature is the presence of multiple jets + high missing transverse energy (MET) + two or more b-jets. The potential background stems from $t\bar{t}$, W + jets, Z^0 + jets and QCD events. An interesting process is the light Higgs-boson h-decay in SUSY processes, $\tilde{q} \rightarrow \tilde{\chi}_2^0 q, \tilde{\chi}_2^0 \rightarrow \tilde{\chi}_1^0 h, h \rightarrow b\bar{b}$, where χ_1^0 and χ_2^0 are neutralinos [4]. The former is stable in R-parity conserving SUSY and therefore leads to a large missing energy.

We have simulated this channel by first requiring from the online trigger and at least 3 jets. In the offline analysis we require more than 5 energetic (> 30 GeV) jets and a missing transverse energy of at least 240 GeV. A relevant parameter is the average direction of particles associated with a high energy jet, in particular its azimuthal angle ϕ transverse to the incident beam directions. The angles $\Delta\phi$ between the direction of the missing energy and those of the two most energetic jets is required to be at least 12°. From measurements of the impact parameters we also keep events with two b-jets. The result is shown in fig. 3.13 which displays the predicted $b\bar{b}$ invariant mass distribution for an integrated luminosity of 100 pb^{-1}, after all cuts. The $h \rightarrow b\bar{b}$ signal (8 ± 1 events) shown by the red histogram is only a small contribution to all SUSY events. The main background stems from $t\bar{t}$ and QCD events, while contributions from W- and Z^0-decays associated with jet production are negligible. For an integrated luminosity of 100 pb^{-1} the significance of the signal peak (43 ± 2 events) is about 8σ.

Figure 3.14 shows the dependence of MET vs. $\Delta\phi$, the angle between the two most energetic jets, for SUSY and QCD events. It appears that, for large missing energies, the two most energetic jets are emitted in opposite directions (large $\Delta\phi$) for QCD events, while for the popular LM1-point of SUSY/mSUGRA they are more isotropically distributed. For the latter there is also a strong correlation between MET and $\Delta\phi$ (green/yellow region in fig. 3.14 left). These features can be used to further decrease the QCD background.

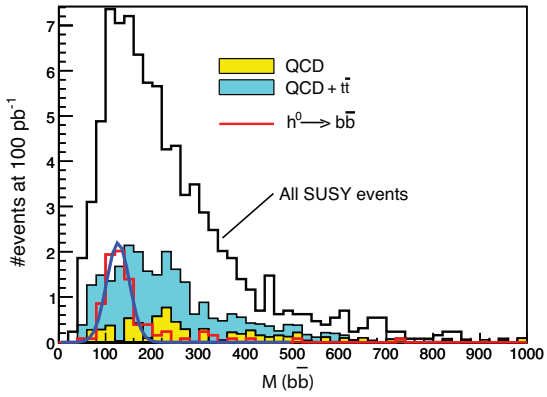

Figure 3.13: *Invariant mass of two b-tagged jets after all selection cuts for SUSY and for background events (simulation). The red curve shows the fit to* $h \rightarrow b\bar{b}$.

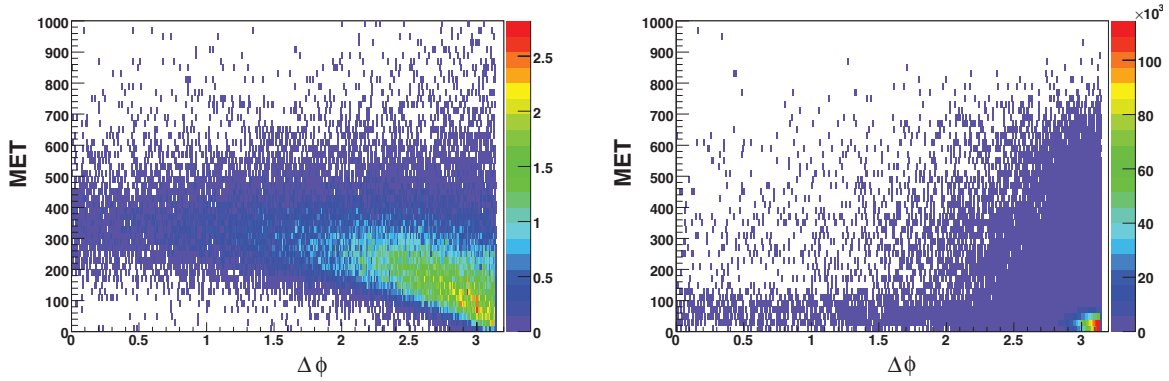

Figure 3.14: *Left:* $\Delta\phi$ *vs. missing transverse energy (MET) for the LM1 point in the mSUGRA parameter space. Right:* $\Delta\phi$ *vs. MET for QCD events (120 <* p_T *< 1000 GeV/c).*

The installation of the pixel detector in CMS is scheduled for May 2008. However, pixel readout tests have already been made in the CMS experimental area with a panel of the endcap pixel detector. Runs with several readout thresholds were recorded for the first time in March 2008 on the CERN TIER 0 storage, using the global CMS data acquisition, and were analyzed with the pixel data quality monitoring software. Results were in line with expectations. Our software codes will be deployed for the global run with the 3.8 T magnetic field scheduled in June 2008, just before LHC is expected to deliver its first beams.

References

[1] Y. Allkofer *et al.*. Nucl. Instrum. Meth. in Phys. Research **A 584** (2008) 25
[2] A. Dorokhov *et al.*, Nucl. Instr. Meth. in Phys. Research **A 530** (2004) 71;
A. Dorokhov *et al.*, Nucl. Instr. Meth. in Phys. Research **A 560** (2006) 112;
V. Chiochia *et al.*, IEEE Trans. Nucl. Sci. **52** (2005) 1067
[3] The CMS collaboration, "CMS Physics Technical Design Report Volume II: Physics Performance", CERN/LHCC 2006-021, CMS TDR 8.2, 2006
[4] F. Moortgat, P. Olbrechts, L. Pape and A. Romeyer, CMS Note 2006/090

4 Publications

Articles

- Design and performance of the silicon sensors for the CMS barrel pixel detector
  Y. Allkofer *et al.*
  Nucl. Instrum. Meth. **A 584** (2008) 25

- A novel aerogel Čerenkov detector for DIRAC-II
  Y. Allkofer *et al.*
  Nucl. Instr. Meth. in Phys. Research **A 582** (2007) 497

- Luminescence quenching of the triplet excimer state by air traces in gaseous argon
  C. Amsler *et al.*
  Journal of Instrumentation **3** (2008) P02001

- CMS Technical Design Report, Volume II : Physics Performance
  CMS Collaboration
  J. Phys. G: Nucl. Part. Phys. **34** (2007) 993

- Protonium production in ATHENA
  L. Venturelli *et al.* (ATHENA Collaboration)
  Nucl. Instr. Meth. in Phys. Research **B 261** (2007) 40

- Production of slow protonium in vacuum
  N. Zurlo *et al.* (ATHENA Collaboration)
  Proc. of the TCP 06 Conf., Hyperfine Int., Springer Verlag, 2007

- Detection of VUV scintillation light in one ton of liquid argon
  C. Regenfus
  Proc. of the 6th Int. Workshop on the Identication of Dark Matter (IDM2006), Rhodes, World Scientific (2007) 325

- Summary of Session 2 : Data Analysis - Algorithms and Tools
  T. Speer
  Proc. of XI Int. Workshop on Advanced Computing and Analysis Techniques in Physics Research, Amsterdam, Proc. of Science, PoS(ACAT) 089 (2007)

- The ATLAS and CMS Detectors and Triggers for B-physics
  T. Speer
  Nucl. Phys. Proc. Suppl. **167** (2007) 221

Articles in press

- A new aerogel Cherenkov detector for DIRAC-II
  Y. Allkofer *et al.*
  Nucl. Instrum. Meth. in Phys. Research **A** (2008)

- The C4F10 Cherenkov detector for DIRAC-II
  S. Horikawa *et al.*
  Nucl. Instrum. Meth. in Phys. Research **A** (2008)

- The CMS Detector at the CERN LHC
  CMS Collaboration
  Journal of Instrumentation (2008)

- The CMS Tracker Operation and Performance at the Magnet Test and Cosmic Challenge
  W. Adam *et al.*
  Journal of Instrumentation (2008)

- Review of Particle Physics
  C. Amsler *et al.* (Particle Data Group)
  To appear in summer 2008

- Quark Model
  C. Amsler, T. DeGrand, B. Krusche
  Review of Particle Physics: to appear in summer 2008

- The $\eta(1405)$, $\eta(1475)$, $f_1(1420)$, and $f_1(1510)$
  C. Amsler and A. Masoni
  Review of Particle Physics: to appear in summer 2008

- Note on scalar mesons
  S. Spanier, N.A. Törnqvist, and C. Amsler
  Review of Particle Physics: to appear in summer 2008

- Partial wave analysis of $\bar{p}p$ annihilation at rest into $2\pi^+2\pi^-\eta$
  C. Amsler *et al.* (Crystal Barrel Collaboration)
  Eur. J. Phys.

- B, D and K decays
  M. Artuso *et al.*
  Eur. J. Phys. (2008), e-Print: arXiv:0801.1833

- Search for πK-atoms with DIRAC II
  Y. Allkofer *et al.*
  Proc. of XII Int. Conf. on Hadron Spectroscopy (Hadron07), Frascati (2007)
  Physics Series, Vol. XLVI (2008)

- V. Chiochia
  The CMS pixel detector: from production to commissioning
  Proc. 10th ICATPP Conf. on Astroparticle, Particle, Space Physics, Detectors and Medical Physics Applications, Como
  e-Print: arXiv:0710.5120 [physics.ins-det]

- B physics at CMS
  T. Speer
  Proc. 2007 Eur. Conf. on High Energy Physics, Manchester
  Journal of Physics: Conference Series

Public Notes

- Lorentz angle calibration for the barrel pixel detector
  Lotte Wilke
  CMS NOTE-2008-012

- A new technique for the reconstruction, validation and simulation of hits in the CMS pixel detector
  M. Swartz *et al.*
  CMS NOTE-2007-033

Invited Lectures

- E. Alagöz
  Turkish Physical Society, Malatya
  29 August 2007
  "Position resolution of the pixel detector for the CMS experiment"

- E. Alagöz
  Swiss Physical Society, Geneva
  27 March 2008
  "Testbeam study of the irradiated pixel barrel sensors for the CMS experiment"

- "Y. Allkofer
  XII Int. Conf. on Hadron Spectroscopy (Hadron07), Frascati
  7 October 2007
  Search for πK-atoms with DIRAC II"

- Y. Allkofer
  CHIPP-plenary meeting, PSI, Villigen
  15 October 2007
  "Search for πK-atoms with DIRAC II"

- V. Boccone
  Swiss Physical Society, Geneva
  26 March 2008
  "Assembly and test of the light readout for the ArDM WIMP-detector"

- V. Chiochia
  10th ICATPP Conf. on Astroparticle, Particle, Space Physics, Detectors and Medical Physics Applications, Como
  10 October 2007
  "The CMS pixel detector: from production to commissioning"

- S. Horikawa
  6th Int. Workshop on Ring Imaging Cherenkov Counters (RICH2007), Trieste
  18 October 2007
  "A new aerogel Cherenkov detector design for DIRAC-II"

- S. Horikawa
  6th Int. Workshop on Ring Imaging Cherenkov Counters (RICH2007), Trieste

19 October 2007
"The DIRAC C4F10 Cherenkov Detector"

- C. Regenfus
Seminar zum Graduiertenkolleg – Physik an Hadron-Beschleunigern, Freiburg i.B.
27 June 2007
"Search for WIMPs with one ton of LAr – the ArDM experiment"

- C. Regenfus
CHIPP-Plenary Meeting, PSI, Villigen
15 October 2007
"Status of the Argon Dark Matter Experiment"

- T. Rommerskirchen
German Physical Society, Freiburg i.B.
5 March 2008
"Study of the discovery potential of supersymmetric final states at CMS"

- T. Rommerskirchen
Swiss Physical Society, Geneva
27 March 2008
"Study of the discovery potential of supersymmetry with final states with missing energy, mutiple jets and b-jets at the CMS detector"

- A. Schmidt
German Physical Society, Freiburg i.B.
5 March 2008
"b-Quark-Jet Identifikation in CMS"

- T. Speer
XI Int. Workshop on Advanced Computing and Analysis Techniques in Physics Research (ACAT), Amsterdam
25 April 2007
"Data analysis and reconstruction algorithms"

- T. Speer
Institute for High Energy Physics of the Austrian Academy of Sciences, Vienna, Austria
22 June 2007
"B-Physics at CMS"

- T. Speer
2007 Eur. Conf. on High Energy Physics, Manchester
20 July 2007
"B-Physics at CMS"

- L. Wilke
Plenary CMS invited talk
21 June 2007
"Flavour Physics"

- L. Wilke
  German Physical Society, Freiburg i.B.
  6 March 2008
  "Lorentz angle calibration for the CMS barrel pixel detector"

ATHENA Collaboration (2007):
M. Amoretti, C. Amsler, G. Bonomi, C. Carraro, C. L. Cesar, M. Charlton, M. Doser, A. Fontana, R. Funakoshi, P. Genova, R. S. Hayano, L. V. Joergensen, A. Kellerbauer, V. Lagomarsino, R. Landua, E. Lodi Rizzini, M. Macri, N. Madsen, G. Manuzio, D. Mitchard, P. Montagna, L. G. Posada, H. Pruys, C. Regenfus, J. Rochet, A. Rotondi, G. Testera, D. P. Van der Werf, A. Variola, L. Venturelli, Y. Yamazaki, N. Zurlo

CRYSTAL BARREL Collaboration (2006):
C. Amsler, C. A. Baker, B. M. Barnett, C. J. Batty, M. Benayoun, P. Blüm, K. Braune, V. Credé, K. M. Crowe, M. Doser, W. Dünnweber, D. Engelhardt, M. A. Faessler, R. P. Haddock, F. H. Heinsius, N. P. Hessey, P. Hidas, D. Jamnik, H. Kalinowsky, P. Kammel, J. Kisiel, E. Klempt, H. Koch, M. Kunze, U. Kurilla, R. Landua, H. Matthäy, C. A. Meyer, F. Meyer-Wildhagen, R. Ouared, K. Peters, B. Pick, M. Ratajczak, C. Regenfus, U. Strohbusch, M. Suffert, U. Thoma, I. Uman, S. Wallis-Plachner, D. Walther, U. Wiedner, B. S. Zou, Č. Zupančič

PARTICLE DATA Group (2006):
W.-M.Yao, C. Amsler, D. Asner, K.S. Babu, R.M. Barnett, J. Beringer, P.R. Burchat, C.D. Carone, C. Caso, O. Dahl, G.D'Ambrosio, A.D. Gouvea, M. Doser, S. Eidelman, J.L. Feng, T. Gherghetta, M. Goodman, C. Grab, D.E. Groom, A. Gurtu, K. Hagiwara, K.G. Hayes, J.J. Hernandez-Rey, K. Hikasa, H. Jawahery, C. Kolda, Y. Kwon, M.L. Mangano, A.V. Manohar, A. Masoni, R. Miquel, K. Mönig, H. Murayama, K. Nakamura, S. Navas, K.A.Olive, L. Pape, C. Patrignani, A. Piepke, G. Punzi, G. Raffelt, J.G. Smith, M. Tanabashi, J. Terning, N.A. Törnqvist, T.G. Trippe, P. Vogel, T. Watari C.G. Wohl, R.L. Workman, P.A. Zyla

DIRAC Collaboration (2008):
B. Adeva, L. Afanas'ev, Y. Allkofer, C. Amsler, D. Bartos, A. Benelli, V. Brekhovskikh, A. Caragheorgheopol, T. Cechak, M. Chiba, S. Constantinescu, C.O. Curceanu, C. Detraz, D. Dreossi, D. Drijard, A. Dudarev, I. Evangelou, J. L. Fungueirino Pazos, J. Gerndt, P. Gianotti, G. Giolu, O. Gorchakov, K. Gritsay, C. Guaraldo, M. Hansroul, S. Horikawa, M. Iliescu, V. Karpukhin, J. Kluson, M. Kobayashi, P. Kokkas, V. Komarov, L. Kruglova, V. Kruglov, A. Kulikov, A. Kuptsov, K. I. Kuroda, A. Lamberto, A. Lanaro, V. Lapchine, R. Lednicky, P. Levi Sandri, L. Lopez Aguera, V. Lucherini, N. Manthos, C. Marinas Pardo, L. Nemenov, M. Nikitin, K. Okada, V. Ol'shevskiy, M. Pentia, A. Penzo, M. Plo, T.C. Ponta, Z. Pustylnik, G.F. Rappazzo, J. Rochet, A. Romero Vidal, J. J. Saborido Silva, J. Schacher, F. Takeutchi, A. Tarasov, L. Tauscher, F. A. Triantis, T. Trojek, S. Trusov, J. Smolik, S. Sugimoto, A. Ryazantsev, V. Rykalin, O. Vazquez Doce, T. Vrba, V. Yaz'kov, M. Zhabitskiy, P. Zrelov